Dalton Transactions

ROYAL SOCIETY OF CHEMISTRY

PAPER

View Article Online
View Journal | View Issue

Cite this: *Dalton Trans.*, 2022, **51**, 14107

Modulation of the structural information in shape-defined heterocyclic strands: the case of a (pyridine-hydrazone)$_2$pyrazine ligand†‡

Muthu Kumar Thangavel, [a,b] Jack Harrowfield, [b] Corinne Bailly,[c] Lydia Karmazin [c] and Adrian-Mihail Stadler *[b,d,e]

Metal ions (Ag^+, Cd^{2+}, Eu^{3+}, Sm^{3+}) and protons can, through coordination and protonation, modulate in three specific ways the structural information contained in the pyrazine-based heterocyclic strand **L** (obtained from 2,5-bis(methylhydrazino)pyrazine and 2 equivalents of 2-pyridinecarboxaldehyde), thus generating two linear rod-like conformations and a bent one. This conformational diversity is associated with a structural one that consists of two diprotonated forms ($H_2\mathbf{L}(PF_6)_2$ and $H_2\mathbf{L}(CF_3SO_3)_2$), a polymeric architecture $[Ag\mathbf{L}]_n(CF_3SO_3)_n$, two rack-like complexes ($[Eu_2H_2\mathbf{L}_3(CF_3SO_3)_6](PF_6)_2$ and $[Sm_2H_2\mathbf{L}_3(CF_3SO_3)_6](PF_6)_2$) and a grid-like structure ($[Cd_4\mathbf{L}_4](CF_3SO_3)_8$).

Received 30th May 2022,
Accepted 22nd August 2022

DOI: 10.1039/d2dt01684b

rsc.li/dalton

Introduction

Of the many metallosupramolecular architectures,[1] those consisting of 4 rod-like, ditopic ligands disposed in orthogonal pairs linked by 4 nodes (mostly metal ions), defining the 4 intersection points of the rods, are termed [2 × 2] grids.[2] The interest in such complexes increases in proportion to the diversification of their chemistry and properties.[2b] Three main types of such architectures can be defined (Fig. 1): classical (or normal) grids, cross grids and alternate grids. While a considerable number of examples of classical grids (type 1) has been synthesised and studied,[2] the cross grids[3] (type 2) and the alternate[4] ones (type 3) are less common. This has provided motivation for the design, synthesis and study of ligands capable of generating cross grids. Such ligands (Fig. 2) should contain a central unit that possesses an inversion centre, for example, like the heterocyclic unit 2,5-disubstituted-pyrazine present in the known cases of **A**, **B** and **D** (Fig. 2), members of a family having sufficient conformational flexibility to enable them to adopt different forms in their free, protonated and co-ordinated states (Fig. 3).

Metal-ion induced conformational changes are relevant to many of the molecular machines and devices reported until now,[5] a particular role in this field being played by hydrazone-based ligands.[6]

In extension of this work, we have explored the coordinative behaviour of ligand **L** (Fig. 4) in the presence of several metal ions, with the aim of understanding how the structural information provided by the ligand can be modulated on interaction with these cations and what are the conformational changes induced by its coordination and protonation (Fig. 3). Ligand **L** has a 2,5-disubstituted-pyrazine as a central unit and two tridentate N_3 sites and was expected to be a good candidate for the selfassembly of [2 × 2] cross grids with metal ions favouring octahedral coordination. Ligand **L** was previously described[7] and it is easily accessible through the reaction of 2,5-bis(methylhydrazino)pyrazine (obtained from 2,5-dibromo-

[a]*Institut de Chimie, Université de Strasbourg, Strasbourg, France*
[b]*Institut de Science et d'Ingénierie Supramoléculaires (ISIS), UMR 7006, CNRS – Université de Strasbourg, 8 Allée Gaspard Monge, 67000 Strasbourg, France. E-mail: mstadler@unistra.fr*
[c]*Service de Radiocristallographie, Université de Strasbourg, 1 Rue Blaise Pascal, 67000 Strasbourg, France*
[d]*University of Strasbourg Institute for Advanced Study (USIAS), 5 Allée du Général Rouvillois, 67083 Strasbourg, France*
[e]*Institut für Nanotechnologie (INT), Karlsruhe Institut für Technologie (KIT), 76344 Eggenstein-Leopoldshafen, Germany*

†Dedicated to Professor Jean-Marie Lehn.

‡CCDC 2171967–2171969 and 2171971–2171973. For crystallographic data in CIF or other electronic format see DOI: https://doi.org/10.1039/d2dt01684b

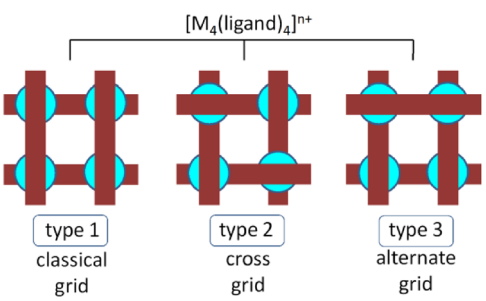

Fig. 1 Three types of [2 × 2] grids generated by ditopic ligands.

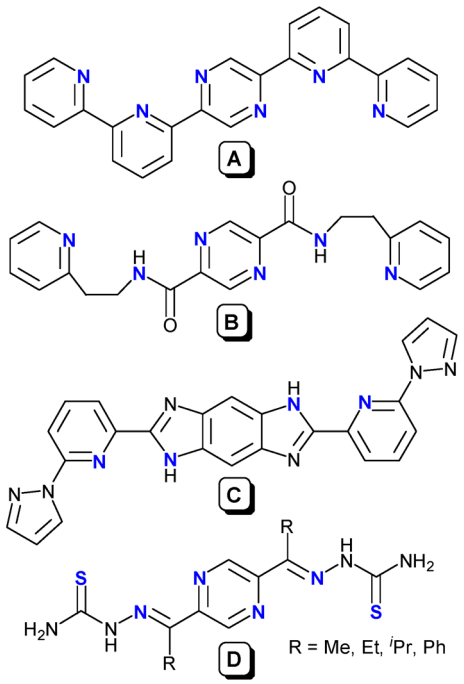

Fig. 2 Structural formulae of ligands A,[3a] B,[3b] C[3c] and D[3d] of which cross grids are already known.

pyrazine and methylhydrazine) with 2 equivalents of 2-pyridinecarboxaldehyde. Its rack-type complex $[Ru_2\mathbf{L}(terpy)_2]^{4+}$ has already been reported.[7] We describe herein the compounds generated by ligand **L** on reaction with the cations Ag^+, H^+, Cd^{2+}, Eu^{3+} and Sm^{3+}. Given evidence of at least partial dissociation in solution, we have limited the present discussion to that of the solid state, on the basis of X-ray structures.

Results and discussion

In anticipation of the formation of complexes with the 1 : 1 metal : ligand stoichiometry of a grid species, ligand **L** was reacted with equimolar amounts of the various metal ions as their triflate ($OTf^- = CF_3SO_3^-$) salts in acetonitrile. The crystalline materials thereby isolated, in some cases after the addition of NH_4PF_6 (see Experimental), proved to correspond to complexes $[Cd_4\mathbf{L}_4](OTf)_8$, $[Ag\mathbf{L}]_n(OTf)_n$, $[Sm_2H_2\mathbf{L}_3(OTf)_6](PF_6)_2$, $[Eu_2H_2\mathbf{L}_3(OTf)_6](PF_6)_2$ and protonated forms $H_2\mathbf{L}(PF_6)_2$ (in the presence of La^{3+}) and $H_2\mathbf{L}(OTf)_2$ (in the presence of Lu^{3+}). The formation of Ln^{3+}-hydroxo species in the presence of aza-aromatic ligands and traces of water is a well known phenomenon[8] and probably explains the presence of partly protonated ligands in the Sm^{3+} and Eu^{3+} species and the isolation simply of the protonated ligand from solutions containing La^{3+} and Lu^{3+}.

It is known that 2,2′-bipyridine preferentially adopts a *s-trans* (transoid) conformation, where the N sp^2 atoms are *anti* oriented,[9] as is also the case for the 2-pyridine-hydrazone unit,[10] and assuming that the same behaviour would be seen in the 2-pyrazine-hydrazone unit and its derivatives, we expected that free ligand **L** would adopt a linear rod-like conformation where the N sp^2 atoms of heterocycles (pyridine and pyrazine) and of hydrazones are in *anti* orientations, as depicted in Fig. 4a. A conformation where the N-donor atoms are *anti* periplanar has been found in 2,5-bis(*N*-pyrazolyl)pyrazine.[11] An outline of the conformational characteristics of ligand **L** in both protonated and metal-ion coordinate forms observed in the present study is given in Fig. 4.

Selected structural data providing detailed support of the idealisations in Fig. 4 are given in Tables 1 and 2. The M–N bond length values given in Table 1 show that the different metal ions have quite distinct preferences for N-donor atoms of the three types present. Thus, while Cd^{2+}, Eu^{3+} and Sm^{3+} all coordinate to pyridine-N (N_{py}), hydrazone-N sp^2 (N_{hyz}) and pyrazine-N (N_{pz}) through tridentate unit bonding, the bond lengths increase in the order $N_{py} < N_{hyz} < N_{pz}$ for Cd^{2+} but in the opposite order for the two lanthanide ions, where discrimination between the three types is significantly less. For Ag^+, N_{py} coordination is strongly preferred over that of N_{hyz} and N_{pz} remains uncoordinated. While some torsion angles (Table 2) vary greatly depending on the interactions of the ligand, the overall form of **L** remains quite close to planar, indicating a significant degree of delocalisation regardless of whether a proton or a metal ion is bound. Representations of the cations present in the crystal structures are given in Fig. 5 (the Eu^{3+} and Sm^{3+} species being isostructural, only that of Eu^{3+} is shown).

Only the tetranuclear complex $[Cd_4\mathbf{L}_4]^{8+}$has the [2 × 2] cross-grid form. It has features of a grid (two orthogonal pairs of linear ligands), as well as of a circular helicate in that the Cd^{2+} centres of a given grid unit can be considered as homochiral (see ahead). The capacity of Cd^{2+} to adopt octahedral coordination (even if irregular) is satisfied by the ligand having a conformation with two oppositely oriented tridentate binding sites involving pyridine-N, pyrazine-N and hydrazone-N donors. Unlike "normal" grids with octahedral metal ions

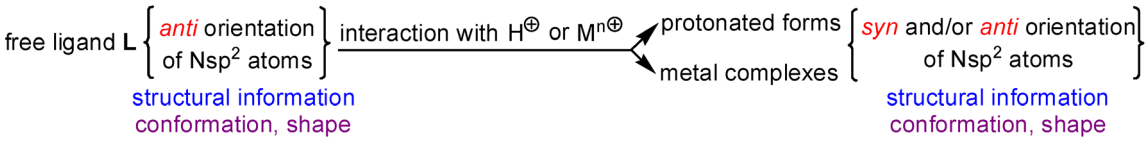

Fig. 3 Simplified scheme showing that the structural information of ligand L – where the relative orientations of N sp^2 atoms play a crucial role – can be modulated upon coordination and protonation, by converting all or some of the *anti* relative orientations of N sp^2 atoms into *syn* orientations.

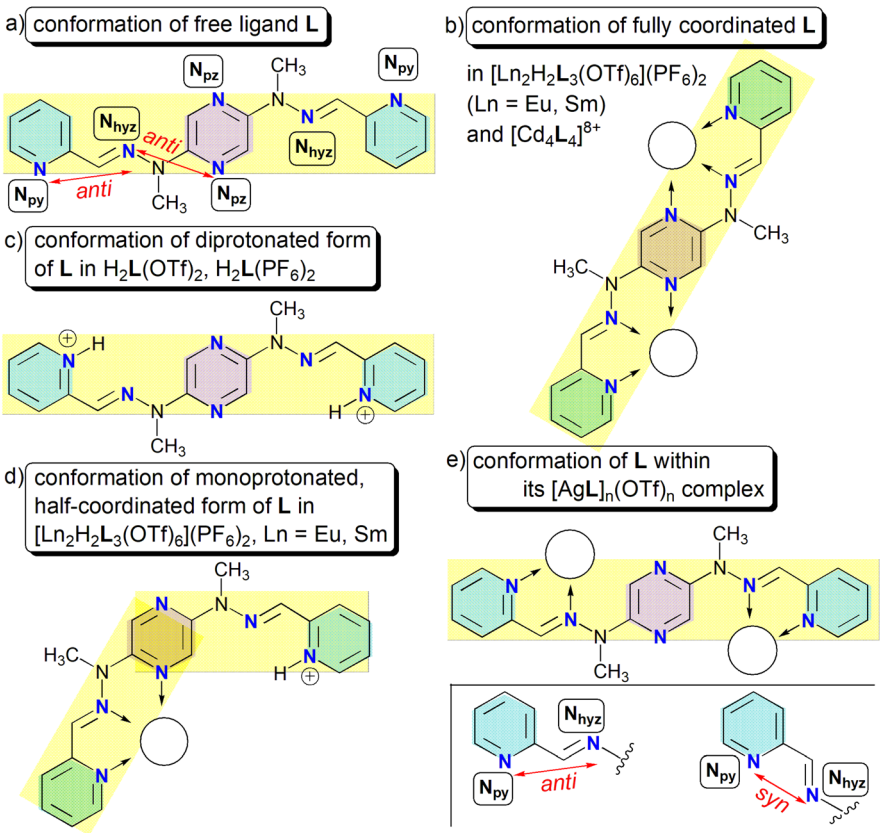

Fig. 4 Structural formulae of ligand L showing the conformations – linear (a, b, c, e) and bent (d) – adopted by the free ligand, as well as upon its coordination and protonation.

Table 1 Bond lengths and atom separations in the protonated forms and metal ion complexes of ligand L

Compound	M···M distance/Å	M–N_{py} distance/Å	M–N_{hyz} distance/Å	M–N_{pz} distance/Å	Ligand length[a]/Å
$H_2L(OTf)_2$	—	—	—	—	18.16(1)
$H_2L(PF_6)_2$	—	—	—	—	18.066(9)
$[Cd_4L_4](OTf)_8$	7.6229(9)	2.291(6); 2.294(6)[b]	2.334(6); 2.356(7)[b]	2.386(6): 2.485(6)[b]	18.075(1)
$[AgL]_n(OTf)_n$	9.0846(4)	2.179(2): 2.180(2)[b]	2.659(2); 2.657(2)[b]	—	18.35(1)
$[Sm_2H_2L_3(OTf)_6](PF_6)_2$	7.865(7)	2.599(4)[c]	2.581(4)[c]	2.566(4)[c]	18.25(1)[c]
		2.590(4)[d]	2.580(4)[d]	2.564(4)[d]	16.44(2)[d]
$[Eu_2H_2L_3(OTf)_6](PF_6)_2$	7.843(7)	2.584(2)[c]	2.572(2)[c]	2.556(2)[c]	18.26(2)[c]
		2.584(2)[d]	2.568(2)[d]	2.554(2)[d]	16.43(2)[d]

[a] Measured as the separation between the 4-position H-atoms of the pyridine rings. [b] Inequivalent donor atom sites. [c] Fully coordinated ligand. [d] Monoprotonated, half-coordinated ligand.

where the binding sites have the same orientation and the metal ion complex corners can be considered as units which alternate in chirality ΔΛΔΛ, so that the complete grid unit is achiral, in cross grids the configurations are either ΔΔΔΔ or ΛΛΛΛ but in the present case both enantiomeric grid units are present in the crystal and it is racemic. The grid units possess helical chirality. The grids lie in racemic sheets parallel to (001) with approach of the terminal pyridine units of the ligands suggestive of some degree of aromatic embrace,[12] although examination of the Hirshfeld surface as obtained with CrystalExplorer[13] shows that any such interactions do not exceed dispersion. Interactions which do exceed dispersion involve a complicated array of aliphatic and aromatic CH···O and CH···F contacts along with aromatic-C···O contacts, all involving the uncoordinated triflate anions, which are distributed both in sheets between those of the grids and within the grid sheets. As is commonly the case with [2 × 2] grids,[2] the Cd_4 array is not exactly square but it is truly planar. Structural details for the grid form are included in Tables 1 and 2 and shown in Fig. 5a. One of the terminal pyridine rings makes an angle of about 3.4° with the pyrazine ring of the same ligand, while the other pyridine ring is almost coplanar with the pyrazine (angle of 0.5°). All N-donor atoms are in a *syn* orientation (Fig. 4b) because of the binding of metal ions to the ligands.

Table 2 Torsion angles/° defining the extent of ligand twisting in the protonated forms and metal ion complexes of ligand **L** (atom numbering as in the figure below)

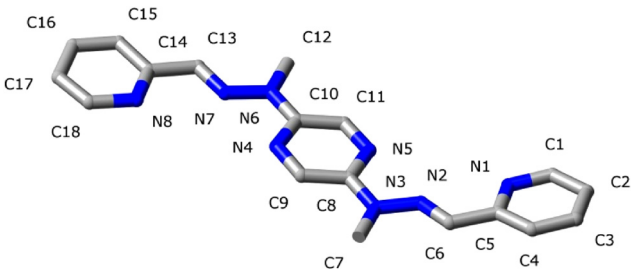

Compound	N1–C5–C6–N2 N8–C14–C13–N7 (py–hyz twist)	N2–N3–C8–N5 N7–N6–C10–N4 (hyz–pz twist)	N1–C5–C8–N5 N8–C14–-C10–N4 (py–pz twist)	N1–C5–C14–N8 (py–py twist)
$H_2\mathbf{L}(OTf)_2$	3.3	172.2	167.6	174.2
	4.1	175.7	171.3	
$H_2\mathbf{L}(PF_6)_2$	2.7[a]	175.1[a]	172.8[a]	180[a]
$[Cd_4\mathbf{L}_4](OTf)_8$	2.1	8.9	3.4	175.4
	1.4	0.1	0.5	
$[Ag\mathbf{L}]_n(OTf)_n$	4.6	164.5	141.7	177.7
	5.2	163.5	137.9	
$[Sm_2H_2\mathbf{L}_3(OTf)_6]$	5.5[b]	176.2[b]	165.3[b]	23.1[b]
$(PF_6)_2$	1.9[b]	14.4[b]	0.6[b]	180[a]
	1.5[a]	2.7[a]	12.4[a]	
$[Eu_2H_2\mathbf{L}_3(OTf)_6]$	6.6[b]	177.1[b]	166.4[b]	22.6[b]
$(PF_6)_2$	2.5[b]	14.7[b]	0.7[b]	180[a]
	0.8[a]	1.7[a]	12.9[a]	

[a] Ligand with two fold symmetry [b] Monoprotonated, half-coordinated ligand, proton on N1.

While the coordination chemistry of Cd^{2+} is characterised by instances of regular coordination geometry, that of Ag^+ would be best said to be typically irregular, with six-coordination being relatively rare,[14] so that it is unsurprising to find that $[AgL]_nOTf_n$, despite its stoichiometry consistent with a grid formulation, does not have such a form. Instead, the structure provides another example of a rather common situation with Ag^+ where two donor atoms form a near linear array with Ag^+ which is perturbed by more remote and presumably weaker interactions. The Hirshfeld surface in fact shows that in addition to two short Ag–N interactions (Ag–N1 2.179(2); Ag–N8 2.180(2) Å) and two longer (Ag–N2 2.657(2); Ag–N7 2.659(2) Å), there are two intermolecular Ag–H interactions (Ag–H9 2.685(1); Ag–H11 2.675(1) Å) that serve to reinforce the polymeric nature of the complex, which forms monoperiodic strands running parallel to [001]. The N1–Ag–N8 unit, bond angle 166.6°, is close to linear while N2–Ag–N7, bond angle 79.7°, is far from it and the AgN_4 unit is very far from tetrahedral. The polymeric nature of the complex results from the fact that one five-membered chelate ring involving pyridine-N1 and hydrazone-N2 is associated with another five-membered chelate formed by pyridine-N8 and hydrazone-N7 from another ligand unit (displacement x, 3.5 − y, z − 0.5), that is, the ligand acts as a divergent, bis (bidentate) bridge. The pyrazine-N atoms are not involved in coordination and the N-donor atoms of the hydrazone and pyrazine units are *anti* oriented, with an average torsion angle of 164°. The separation between Ag^+ ions within the polymer is 9.0846(4) Å (Fig. 5b). The triflate counteranion is not involved in coordination to Ag^+ and appears to be predominantly involved in CH···O contacts. Unlike the near-planar bis(tridentate) form of the ligand found with Cd^{2+}, the ligand in its Ag^+ complex shows an appreciable twist about the pyrazine core, with torsion angles close to 164° about the pyrazine-hydrazone bond. Other structural details are given in Tables 1 and 2.

The complexes $[Eu_2H_2\mathbf{L}_3(OTf)_6](PF_6)_2$ and $[Sm_2H_2\mathbf{L}_3(OTf)_6](PF_6)_2$ are isostructural, not unexpectedly given that Sm and Eu are adjacent members of the lanthanide series (although that is no guarantee !), so that we discuss only the slightly more precise determination, that of the Eu^{3+} complex. Again, given the characteristics of Ln^{3+} (lanthanide(III)) coordination chemistry[15] such as oxophilicity, high coordination numbers and a lack of strong stereochemical preferences, it was not to be expected that a basic ligand designed for grid formation with octahedral metal ions would necessarily give lanthanide grids. Nonetheless, unlike Ag^+, Eu^{3+} does bind to tridentate ligand pockets involving pyridine-, hydrazone- and pyrazine-N sp^2 donors and one ligand unit does bind in a bis(tridentate) mode to create a binuclear entity similar to one strut of the Cd^{2+} grid (Fig. 5c). However, there is no further aggregation of these Eu_2 rods and instead the coordination sphere of each metal ion is completed by binding to one tridentate pocket of a singly-protonated ligand and three triflate-O donors, making each Eu 9-coordinate in an N_6O_3 environment (Fig. 4 and 5). As noted above, it is presumed that the ligand protonation is a result of lanthanide aqua ion hydrolysis ($[Eu\text{-}OH_2]^{3+}$ + L → [Eu-

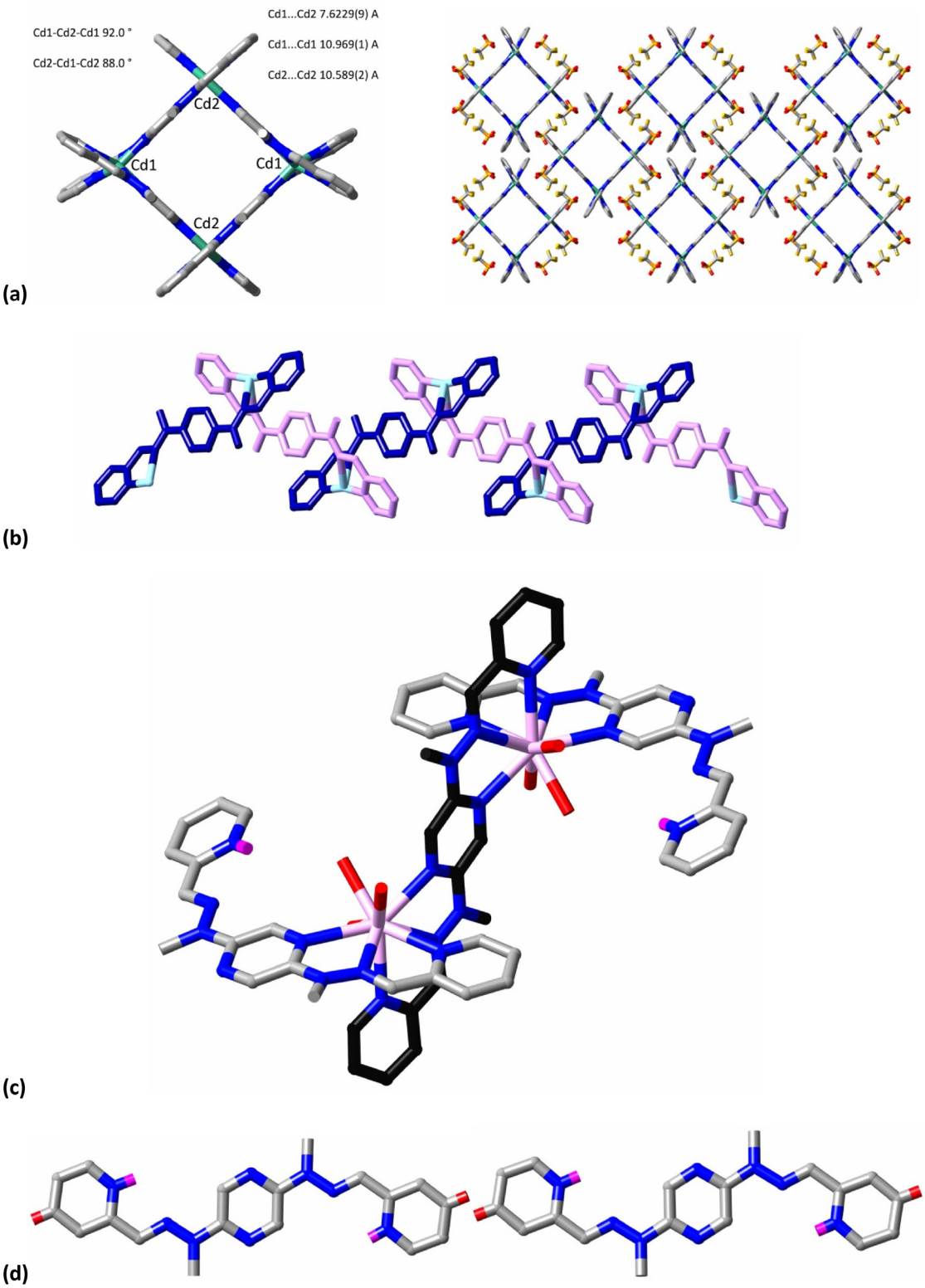

Fig. 5 Stick representations of the species present in the different structures: (a) (left) $[Cd_4L_4]^{8+}$ and its dimensions; (right) part of one sheet of the grid cations and the triflate anions which lie within this sheet and occupy the space between but not within the cations. H-Atoms are not shown; (b) part of the helical polymer units found in the structure of $[AgL]_n(OTf)_n$, with all atoms of ligand units shown alternately in dark blue or pink; Ag = light blue, the very irregular nature of its N_4 coordination sphere being apparent; neither the counteranions nor H-atoms are shown; (c) perspective view of the cation present in the structure of $[Eu_2H_2L_3(OTf)_6](PF_6)_2$, with carbon atoms of the fully coordinated ligand shown in black and only the protons bound to pyridine-N of the half-coordinated ligands shown in bright pink. Only the bound O-atoms (red) of the partially disordered triflate ligands are shown and the $[PF_6]^-$ anions are not shown; Eu = light pink; (d) the virtually identical dications present in $H_2L(OTf)_2$ (left) and $H_2L(PF_6)_2$ (right), with the protons on pyridine-N shown in bright pink and those used as points to define the length of the ligand in red. Counteranions are not shown.

OH]$^{2+}$ + LH^{+}). The proton has been located on the pyridine-N and it may be its involvement in H-bonding to an uncoordinated triflate-O atom (NH1···O6 2.07 Å) that explains the limited effect of this monoprotonation, like that on 2,2′;6′,2″-terpyridine,[16] where monoprotonation also leads to a *syn–anti* orientation of the N-donors. The monoprotonated ligand has a convergent arrangement of the H^{+} and Eu^{3+} binding sites, whereas the two Eu^{3+} sites are divergent for the unprotonated form but in both cases the ligand remains close to planar, with only small degrees of twisting of the terminal pyridine rings from the plane of the pyrazine core (Table 2). A limited capacity of the bis(tridentate) form of **L** to accommodate different metal ions is seen in the M···M distances of 7.843(9) Å (M = Eu), 7.865(9) Å (M = Sm) and 7.6229(9) Å (M = Cd).

The cations present in the two diprotonated ligand salts H_2**L**$(OTf)_2$ and H_2**L**$(PF_6)_2$, isolated from attempts to obtain the Lu^{3+} and La^{3+} complexes, respectively, are essentially identical in form, with the protons located on the two terminal pyridine rings and the ligand conformations being very close to planar. As in the monoprotonated ligand bound to Eu^{3+} or Sm^{3+}, protonation of the pyridine-N results only in conversion of the pyridine-N and hydrazone-N into a cisoid arrangement (Fig. 4c and 5d). Analysis of the cation–anion interactions in the crystals is simpler in the case of H_2**L**$(PF_6)_2$, (Fig. 6) where there is no disorder of the anions. Here, consideration of the Hirshfeld surface shows that one reason why the pyrazine-N does not adopt a cisoid conformation relative to the hydrazone-N is because acetonitrile–N···H interactions bridge the pyridine-NH and CH adjacent to pyrazine-N (H1N···N5 2.15 Å; H9···N5 2.57 Å). Aromatic-CH···FP contacts (H4···F3 2.47 Å; H6···F4 2.34 Å) also influence the solid state conformation, appearing to favour a planar form. In H_2**L**$(OTf)_2$, triflate-O plays both roles.

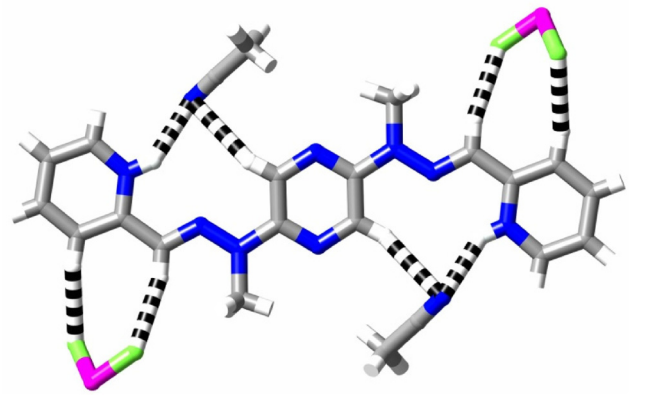

Fig. 6 Weak interactions (dashed lines) in the crystal of H_2**L**$(PF_6)_2$ (colour code H = white, C = grey, N = blue, F = pale green, P = violet).

Within both the diprotonated and monoprotonated ligands, the H^{+} cation is located on the N_{py} atom of pyridine rings, which is the most basic among N_{py}, N_{pz} and N_{hyz}. In all these structures, the N_{hyz} and N_{pz} atoms are in a *syn* periplanar orientation with $N_{hyz}C–CN_{pz}$ torsion angles between 0.7° and 6.6° (Table 2). The same orientation is found in other ligands that contain a protonated pyridine-hydrazone motif,[17] as well as in monoprotonated 2,2′-bipyridine.[18] The N_{py}–H bond lengths lie between 0.8 Å and 0.9 Å, while the N_{hyz}···H distances lie between 2.3 Å and 2.4 Å with quite acute N_{py}–H···N_{hyz} angles close to 100°, indicating that any H-bonding interaction must be rather weak.

One can summarise the conformational and shape changes seen in the present structures (see also Table 3):

(a) Interaction of **L** with singly charged cations (Ag^{+}, H^{+}) results in conformations where the three N atoms of a tridentate N_3 site are oriented as follows (for the corresponding torsion angles, see Table 2): (i) N_{py} and N_{hyz} atoms are *syn* periplanar (Sp), and (ii) N_{hyz} and N_{pz} atoms are *anti* periplanar (Ap). These Sp-Ap-Ap-Sp conformations are present in compounds H_2**L**$(OTf)_2$, H_2**L**$(PF_6)_2$ and [Ag**L**]$_n(OTf)_n$. The monocharged cations Ag^{+} and H^{+} induce similar conformational changes despite their very different binding character.

(b) Binding of two doubly (Cd^{2+}) or triply (Eu^{3+}, Sm^{3+}) charged metal ions to one molecule of ligand **L** produces the conversion of all *anti* periplanar orientations of the N-donor atoms (Ap-Ap-Ap-Ap) into *syn* periplanar conformations (Sp-Sp-Sp-Sp). From a formal point of view, the conformational changes of the ligand **L** can be seen as a displacement of 60°

Table 3 Modulation of structural information: conformational consequences induced by the orientation of N sp^2 atoms in compounds of ligand **L** with respect to free ligand (Ap = *anti* periplanar, Sp = *syn* periplanar)

Compound	First type of N_3 site		Second type of N_3 site		Conformational consequences of binding of H^{+} or M^{n+} to **L**
	N_{py}/N_{hyz}	N_{hyz}/N_{pz}	N_{pz}/N_{hyz}	N_{hyz}/N_{py}	
L	Ap	Ap	Ap	Ap	—
H_2**L**$(OTf)_2$	Sp	Ap	Ap	Sp	180° rotation of terminal pyridine rings
H_2**L**$(PF_6)_2$	Sp	Ap	Ap	Sp	
[Ag**L**]$_n(OTf)_n$	Sp	Ap	Ap	Sp	
$[Cd_4L_4]^{8+}$	Sp	Sp	Sp	Sp	Rotation of pyridines and hydrazones
$[Eu_2H_2L_3(OTf)_6](PF_6)_2$ $[Sm_2H_2L_3(OTf)_6](PF_6)_2$ fully coordinated	Sp	Sp	Sp	Sp	
$[Eu_2H_2L_3(OTf)_6](PF_6)_2$ $[Sm_2H_2L_3(OTf)_6](PF_6)_2$ monoprotonated, half-coordinated	Sp	Sp	Ap	Sp	Contraction of **L** with an amplitude of about 1.7 Å, resulting in a bent conformation of **L**

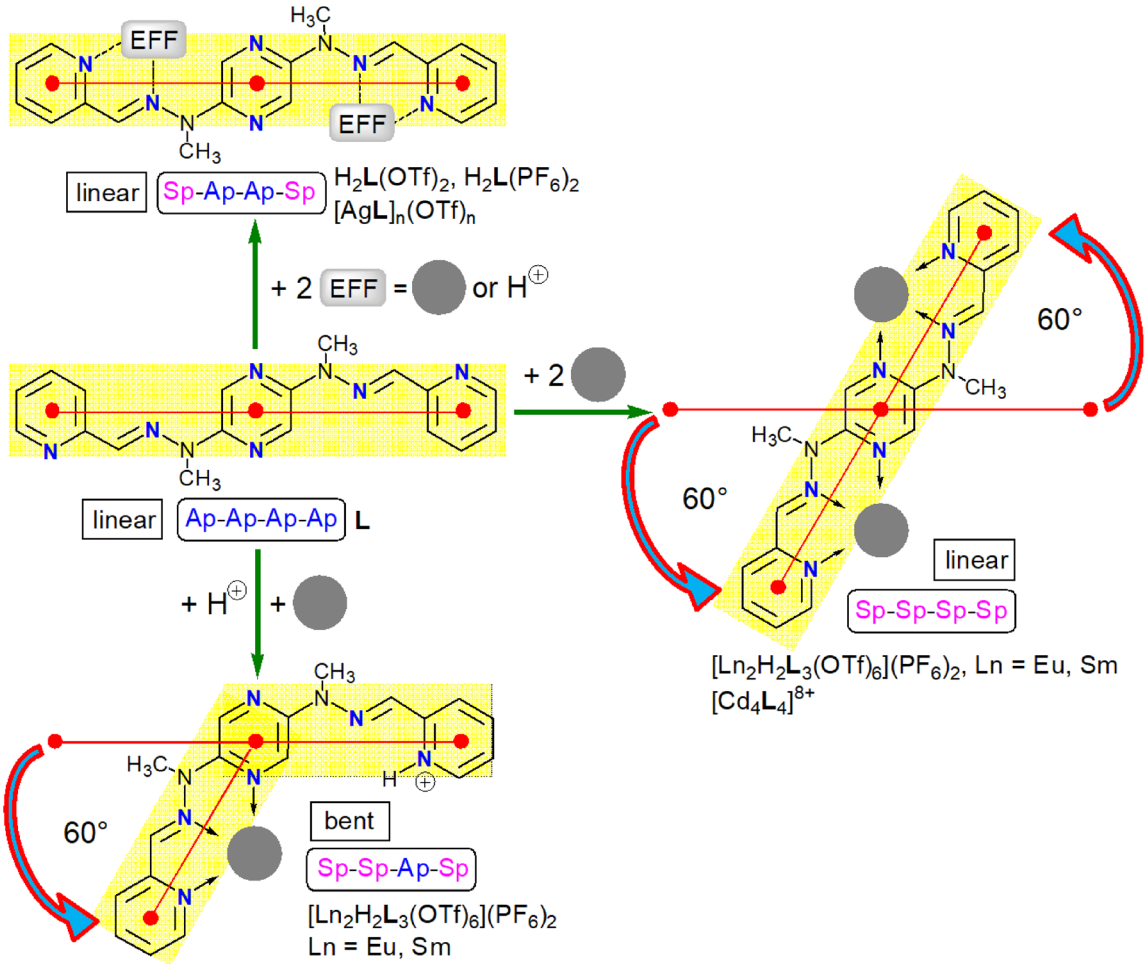

Fig. 7 Representation of the motion of pyridine-hydrazone units with respect to the pyrazine ring. On reaction with the appropriate effectors, the Ap-Ap-Ap-Ap conformation (linear shape) of the free ligand is converted to Sp-Sp-Sp-Sp (linear), Sp-Ap-Ap-Sp (linear) and Sp-Sp-Ap-Sp (bent) conformations. Sp = *syn* periplanar, Ap = *anti* periplanar.

of the center of pyridine rings in the plane of pyrazine and with respect to the center of pyrazine ring[19] (Fig. 7).

(c) In all complexes considered under (a) and (b), the overall shape of the ligand remains fully extended, with a length between 17.7 Å and 18.2 Å, expected to be close to the length of free ligand.

(d) The monoprotonated, half coordinated ligands have one N_3 site occupied with a Ln^{3+} cation, while the other N_3 site hosts a H^+ atom at the on the N_{py} atom. This induces significant bending and a contraction in length of about 1.6 Å with respect to the fully coordinated ligand (Table 1). Here, the Ap-Ap-Ap-Ap linear conformation is converted to a bent Sp-Sp-Ap-Sp conformation (Fig. 7 and Table 3), present in complexes $[Eu_2H_2L_3(OTf)_6](PF_6)_2$ and $[Sm_2H_2L_3(OTf)_6](PF_6)_2$.

Conclusions

The ligand **L** has a versatile coordinative behaviour reflecting both the disposition and exact nature of its N-donor atoms and can generate several types of compounds that include diprotonated forms, a coordination polymer and rack-like complexes, as well as a grid-like complex. Although of limited flexibility, it can respond to the particular proclivities of a variety of metal ions. As a cation which favours octahedral coordination, Cd^{2+} does indeed give a cross grid with **L**, indicating that **L** could give rise to an extensive family of such complexes endowed with chirality as a novel characteristic.

Protonation of **L** with 2 equivalents of acid produces conformational changes consisting of rotation of terminal pyridine rings without modification of the essentially rod-like shape of the ligand. Similar conformational changes occur on reaction with Ag^+ cation. From this point of view, H^+ and Ag^+ ions work as equivalent effectors. These findings could be used for the design of novel H^+-based molecular motional devices.[20]

Partial coordination with Ln^{3+} combined with partial protonation[21] leads to a bent/contracted shape of the ligand. Although a fortuitous discovery, this observation is an example of the use of protonation for control of the binding modes of sophisticated ligands.

Table 4 Crystal data and structure refinement details

Compound	$H_2\mathbf{L}(OTf)_2$	$H_2\mathbf{L}(PF_6)_2$	$[Ag\mathbf{L}]_n(OTf)_n$	$[Cd_4\mathbf{L}_4](OTf)_8$
Formula	$C_{20}H_{20}F_6N_8O_6S_2$	$C_{22}H_{26}F_{12}N_{10}P_2$	$C_{19}H_{18}AgF_3N_8O_3S$	$C_{78}H_{72}Cd_4F_{18}N_{32}O_{18}S_6$
M/g mol^{-1}	646.56	720.47	603.34	2729.63
Cryst. syst.	Monoclinic	Monoclinic	Monoclinic	Orthorhombic
T/K	173(2)	120(2)	173(2)	173(2)
Space group	$P2_1/c$	$P2_1/c$	$P2_1/c$	*Ibam*
a/Å	13.2444(4)	8.3460(2)	13.1904(3)	19.2681(9)
b/Å	9.4288(3)	8.6291(2)	13.6729(4)	24.4819(12)
c/Å	21.4191(7)	22.2086(6)	12.2821(4)	26.1478(12)
α/°	90	90	90	90
β/°	92.334(2)	112.091(1)	93.048(2)	90
γ/°	90	90	90	90
V/Å^3	2672.57(15)	1482.77(6)	2211.96(11)	12 334.4(10)
Z	4	2	4	4
Reflns colld	33 776	16 584	59 931	129 852
Indep. reflns	4701	2617	6519	7634
Reflns obs. ($I > 2\sigma(I)$)	3337	2459	4769	4585
R_{int}	0.0810	0.0425	0.0605	0.1012
Params refined	389	214	318	341
R_1	0.0776	0.0444	0.0467	0.0938
wR_2	0.2057	0.1140	0.1080	0.2404
S	1.063	1.063	1.030	1.082
$\Delta\rho_{min}$/e Å^{-3}	−0.691	−0.456	−1.077	−1.347
$\Delta\rho_{max}$/e Å^{-3}	0.894	0.656	2.662	1.553
CCDC	2171971	2171972	2171967	2171968

Compound	$[Eu_2H_2\mathbf{L}_3(OTf)_6](PF_6)_2$	$[Sm_2H_2\mathbf{L}_3(OTf)_6](PF_6)_2$
Formula	$C_{72}H_{74}Eu_2F_{30}N_{30}O_{18}P_2S_6$	$C_{72}H_{74}F_{30}N_{30}O_{18}P_2S_6Sm_2$
M/g mol^{-1}	2775.83	2772.61
Cryst. syst.	Triclinic	Triclinic
T/K	120(2)	120(2)
Space group	$P\bar{1}$	$P\bar{1}$
a/Å	12.5676(7)	12.5735(5)
b/Å	14.0097(6)	13.9962(6)
c/Å	15.1758(9)	15.1959(6)
α/°	100.556(2)	100.481(2)
β/°	96.448(2)	96.634(2)
γ/°	91.114(2)	91.020(2)
V/Å^3	2607.9(2)	2609.90(19)
Z	1	1
Reflns colld	204 125	78 880
Indep. reflns	18 098	9172
Reflns obs. ($I > 2\sigma(I)$)	16 377	8788
R_{int}	0.0498	0.0633
Params refined	767	761
R_1	0.0429	0.0504
wR_2	0.1017	0.1240
S	1.075	1.034
$\Delta\rho_{min}$/e Å^{-3}	−1.820	−0.888
$\Delta\rho_{max}$/e Å^{-3}	2.415	2.474
CCDC	2171969	2171973

Experimental

Synthesis Complex $[Cd_4L_4](CF_3SO_3)_8$

To a suspension of ligand **L** (1.78 mg, 0.0051 mmol, 1 equiv.) in acetonitrile was added $Cd(CF_3SO_3)_2{\cdot}6DMSO$ (4.52 mg, 0.0051 mmol, 1 equiv.) in acetonitrile, the total volume of acetonitrile being of 1.5 mL. The reaction mixture was stirred at room temperature for 10 minutes.

Complex $[AgL]_n(CF_3SO_3)_n$

To a suspension of ligand **L** (2.72 mg, 0.0079 mmol, 1 equiv.) in acetonitrile was added $AgCF_3SO_3$ (2.02 mg, 0.0079 mmol, 1 equiv.) in acetonitrile, the total volume of acetonitrile being of 1.5 mL. The reaction mixture was stirred at room temperature for 10 minutes.

Complex $[Eu_2H_2L_3(CF_3SO_3)_6](PF_6)_2$

To a suspension of ligand **L** (1.03 mg, 0.0029 mmol, 1 equiv.) in acetonitrile was added $Eu(CF_3SO_3)_3$ (1.78 mg, 0.0029 mmol, 1 equiv.) in acetonitrile, the total volume of acetonitrile being of 1.5 mL. The reaction mixture was stirred at room temperature for 10 minutes. Then was added NH_4PF_6 (1.45 mg, 0.0087 mmol, 3 equiv.).

Complex $[Sm_2H_2L_3(CF_3SO_3)_6](PF_6)_2$

To a suspension of ligand **L** (1.57 mg, 0.0045 mmol, 1 equiv.) in acetonitrile was added $Sm(CF_3SO_3)_3$ (2.71 mg, 0.0045 mmol, 1 equiv.) in acetonitrile, the total volume of acetonitrile being of 1.5 mL. The reaction mixture was stirred at room tempera-

ture for 10 minutes. Then was added NH_4PF_6 (2.22 mg, 0.0135 mmol, 3 equiv.).

Protonated form $H_2L(CF_3SO_3)_2$

To a suspension of ligand **L** (1.20 mg, 0.0035 mmol, 1 equiv.) in acetonitrile was added $Lu(CF_3SO_3)_3$ (2.16 mg, 0.0035 mmol, 1 equiv.) in acetonitrile, the total volume of acetonitrile being of 1.5 mL. The reaction mixture was stirred at room temperature for 10 minutes.

Protonated form $H_2L(PF_6)_2$

To a suspension of ligand **L** (1.25 mg, 0.0036 mmol, 1 equiv.) in acetonitrile was added $La(CF_3SO_3)_3$ (2.12 mg, 0.0036 mmol, 1 equiv.) in acetonitrile, the total volume of acetonitrile being of 1.5 mL. The reaction mixture was stirred at room temperature for 10 minutes. Then was added NH_4PF_6 (1.76 mg, 0.0108 mmol, 3 equiv.).

Crystal structure determinations

Single crystals suitable for X-ray diffraction were obtained by slow vapor diffusion of diisopropyl ether into acetonitrile solutions of the complexes or protonated forms.

For the crystal structure determinations, the crystals were placed in oil, and a single crystal was selected, mounted on a glass fiber and placed in a low-temperature N_2 stream. The corresponding crystal data are given in Table 4.

Within the structure of complex $[Eu_2H_2\mathbf{L}_3(OTf)_6](PF_6)_2$, the atoms S1, O2, O3, C28, F1, F2, F3, O5, C29, F4, F5, F6, F7, F8, F9, P1, F10, F11, F12, F13, F14, F15 are disordered over two positions. The atoms S1, O2, O3, C28, F1, F2, F3 of the first triflate are disordered over two positions with an occupancy ratio of 0.55/0.45. The atoms O5, C29, F4, F5, F6 of the second triflate are disordered over two positions with an occupancy ratio of 0.55/0.45. The fluorines F7, F8, F9 of the third triflate are disordered over two positions with an occupancy ratio of 0.50/0.50. The atoms P1, F10, F11, F12, F13, F14, F15 of the hexafluorophosphate anion are disordered over two positions with an occupancy ratio of 0.70/0.30.

Within the structure of complex $[Cd_4\mathbf{L}_4](OTf)_8$, the atoms O5, F4, S2, Cd1, Cd2 are in a special position (population 50%). A squeeze was done. The residual electron density was assigned to a half molecule of triflate and two molecules of DMSO. The squeezed half molecule of triflate was placed in the center of the grid, but was too restless to be correctly modelised.

Within the structure of complex $[Sm_2H_2\mathbf{L}_3(OTf)_6](PF_6)_2$, the atoms C28, C29, O2, O3, O5, O6, F1, F2, F3, F4, F5, F6, F7, F8, F9, F10, F12, F14, F15, S2 are disordered over two positions. The atoms C28, F1, F2, F3 of the first triflate are disordered over two positions with an occupancy ratio of 0.50/0.50. The atoms O2, O3 of the first triflate are disordered over two positions with an occupancy ratio of 0.55/0.45. The atoms S2, O5, O6, C29, F4, F5, F6 of the second triflate are disordered over two positions with an occupancy ratio of 0.50/0.50. The fluorine atoms F7, F8, F9 of the third triflate are disordered over two positions with an occupancy ratio of 0.50/0.50. The fluorine atoms F10, F12, F14, F15 of the hexafluorophosphate anion are disordered over two positions with an occupancy ratio of 0.70/0.30.

Within the structure of protonated form $H_2\mathbf{L}(OTf)_2$, the atoms C20, F4, F5, F6, O5, O6 of the second triflate are disordered over two positions with an occupancy ratio of 0.50/0.50.

Conflicts of interest

There are no conflicts to declare.

Acknowledgements

M. K. T. thanks the LabEx Chimie des Systèmes Complexes (Project Structural and magnetic modulation of polymetallic nano-architectures) for fiancial support. A.-M. S. thanks the University of Strasbourg Institute for Advanced Studies USIAS (Project Molecular machines with multiple mechanical functions).

References

1 For a selection of recent papers, see: (*a*) A. Ahmedova, Biomedical Applications of Metallosupramolecular Assemblies – Structural Aspects of the Anticancer Activity, *Front. Chem.*, 2018, **6**, 620; (*b*) L. Sosa-Vargas, E. Kim and A.-J. Attias, Beyond "decorative" 2D supramolecular self-assembly: strategies towards functional surfaces for nanotechnology, *Mater. Horiz.*, 2017, **4**, 570–583; (*c*) H. Wang, Y. Li, N. Li, A. Filosa and X. Li, Increasing the size and complexity of discrete 2D metallosupramolecules, *Nat. Rev. Mater.*, 2021, **6**, 145–167.

2 For reviews, see: (*a*) M. Ruben, J. Rojo, F. J. Romero-Salguero, L. H. Uppadine and J.-M. Lehn, Grid–Type Metal Ion Architectures: Functional Metallosupramolecular Arrays, *Angew. Chem., Int. Ed.*, 2004, **43**, 3644–3662; (*b*) J. G. Hardy, Metallosupramolecular grid complexes: towards nanostructured materials with high-tech applications, *Chem. Soc. Rev.*, 2013, **42**, 7881–7899; (*c*) A.-M. Stadler, Grids with Unusual, High Nuclearity – A Structural Approach, *Eur. J. Inorg. Chem.*, 2009, 4751–4770; (*d*) L. N. Dawe, K. V. Shuvaev and L. K. Thompson, Polytopic ligand-directed self-assembly-polymetallic [n×n] grids versus non-gridoligomers, *Chem. Soc. Rev.*, 2009, **38**, 2334–2359; (*e*) M. Barboiu, A.-M. Stadler and J.-M. Lehn, Controlled Folding, Motional, and Constitutional Dynamic Processes of Polyheterocyclic Molecular Strands, *Angew. Chem., Int. Ed.*, 2016, **55**, 4130–4154.

3 (*a*) T. Bark, M. Düggeli, H. Stoeckli-Evans and A. von Zelewsky, Designed Molecules for Self-Assembly: The Controlled Formation of Two Chiral Self-Assembled Polynuclear Species with Predetermined Configuration, *Angew. Chem., Int. Ed.*, 2001, **40**, 2848–2851;

(*b*) J. Hausmann and S. Brooker, Control of molecular architecture by use of the appropriate ligand isomer: a mononuclear "corner-type" versus a tetranuclear [2 × 2] grid-type cobalt(III) complex, *Chem. Commun.*, 2004, 1530–1531; (*c*) B. Schäfer, J.-F. Greisch, I. Faus, T. Bodenstein, I. Salitros, O. Fuhr, K. Fink, V. Schünemann, M. M. Kappes and M. Ruben, Divergent Coordination Chemistry: Parallel Synthesis of [2 × 2] Iron(II) Grid-Complex Tauto-Conformers, *Angew. Chem., Int. Ed.*, 2016, **55**, 10881–10885; (*d*) N. Arefyeva, A. Sandleben, A. Krest, U. Baumann, M. Schäfer, M. Kempf and A. Klein, [2 × 2] Molecular Grids of Ni(II) and Zn(II) with Redox-Active 1,4-Pyrazine-Bis(thiosemicarbazone) Ligands, *Inorganics*, 2018, **6**, 51.

4 (*a*) M. Barboiu, F. Dumitru, E. Petit, Y.-M. Legrand and A. V. D. Lee, Mesomeric metallosupramolecular grid architectures, *Supramol. Chem.*, 2015, **27**, 393–400; (*b*) E. Day, B. Kauffmann, M. Scarpi-Luttenauer, A. Chaumont, M. Henry and P. Mobian, An Alternate [2 × 2] Grid Constructed Around TiO_4N_2 Units, *Chem. – Eur. J.*, 2022, **19**, e202200047.

5 For a selection of reviews, see: (*a*) V. Balzani, A. Credi, F. M. Raymo and J. F. Stoddart, Artificial Molecular Machines, *Angew. Chem., Int. Ed.*, 2000, **39**, 3348–3391; (*b*) E. R. Kay, D. A. Leigh and F. Zerbetto, Synthetic molecular motors and mechanical machines, *Angew. Chem., Int. Ed.*, 2007, **46**, 72–191; (*c*) B. Champin, P. Mobian and J.-P. Sauvage, Transition metal complexes as molecular machine prototypes, *Chem. Soc. Rev.*, 2007, **36**, 358–366; (*d*) S. Erbas-Cakmak, D. A. Leigh, C. T. McTernan and A. L. Nussbaumer, Artificial Molecular Machines, *Chem. Rev.*, 2015, **115**, 10081–10206; (*e*) A. Goswami, S. Saha, P. K. Biswas and M. Schmittel, (Nano)mechanical Motion Triggered by Metal Coordination: from Functional Devices to Networked Multicomponent Catalytic Machinery, *Chem. Rev.*, 2019, **120**, 125–199.

6 X. Su and I. Aprahamian, Hydrazone-based switches, metallo-assemblies and sensors, *Chem. Soc. Rev.*, 2014, **43**, 1963–1981.

7 A.-M. Stadler, F. Puntoriero, F. Nastasi, S. Campagna and J.-M. Lehn, Ru(II) multinuclear metallosupramolecular rack-type architectures of polytopic hydrazone-based ligands: synthesis, structural features, absorption spectra, redox behavior, and near-infrared luminescence, *Chem. – Eur. J.*, 2010, **16**, 5645–5660.

8 S. A. Cotton, J. M. Harrowfield, L. Semenova, B. W. Skelton, A. N. Sobolev and A. H. White, Allan White and Polypyridines: Extending the Lanthanide(III) Complex Series, *Aust. J. Chem.*, 2020, **73**, 434–446.

9 A. Göller and U.-W. Grummt, Torsional barriers in biphenyl, 2,2′-bipyridine and 2-phenylpyridine, *Chem. Phys. Lett.*, 2000, **321**, 399–405.

10 K. M. Gardinier, R. G. Khoury and J.-M. Lehn, Enforced Helicity: Efficient Access to Self-Organized Helical Molecular Strands by the Imine Route, *Chem. – Eur. J.*, 2000, **6**, 4124–4131.

11 N. Pizarro, G. Prado, M. Saldías, C. Sandoval-Altamirano and A. Vega, The Effect of Pyrazolyl Substituents on the Photophysical and Photochemical Properties of Pyrazine Derivatives, *Photochem. Photobiol.*, 2018, **94**, 845–852.

12 A. J. Edwards, C. F. McKenzie, P. R. Spackman, D. Jayatilaka and M. A. Spackman, Intermolecular interactions in molecular crystals: what's in a name?, *Faraday Discuss.*, 2017, **203**, 93–112.

13 P. R. Spackman, M. J. Turner, J. J. McKinnon, S. K. Wolff, D. J. Grimwood, D. Jayatilaka and M. A. Spackman, CrystalExplorer: a program for Hirshfeld surface analysis, visualization and quantitative analysis of molecular crystals, *J. Appl. Crystallogr.*, 2021, **54**, 1006–1011.

14 T. C. W. Mak and X.-L. Zhao, Silver: Inorganic & Coordination Chemistry. Based in part on the article Silver: Inorganic & Coordination Chemistry, ed. W. Ewen Smith in *the Encyclopedia of Inorganic Chemistry, First Edition*, 2011, DOI: **10.1002/9781119951438.eibc0205**.

15 S. A. Cotton and J. Harrowfield, Lanthanide Coordination Chemistry, in *The Rare Earth Elements: Fundamentals and Applications*, ed. D. A. Atwood, John Wiley & Sons, Ltd, Chichester, UK, 2012, pp. 73–81.

16 A. Hergold-Brundic, Z. Popovic and D. Matkovic-Calogovic, 2,2′:6′,2″-Terpyridinium Trifluoromethanesulfonate, [terpyH]CF_3SO_3, *Acta Crystallogr., Sect. C: Cryst. Struct. Commun.*, 1996, **52**, 3154–3157, DOI: **10.1107/S0108270196009584**.

17 (*a*) N. Giuseppone, J.-L. Schmitt and J.-M. Lehn, Driven Evolution of a Constitutional Dynamic Library of Molecular Helices Toward the Selective Generation of [2 × 2] Gridlike Arrays under the Pressure of Metal Ion Coordination, *J. Am. Chem. Soc.*, 2006, **128**, 16748–16763; (*b*) D. J. Hutchinson, L. R. Hanton and S. C. Moratti, Control of Self-Assembly through the Influence of Terminal Hydroxymethyl Groups on the Metal Coordination of Pyrimidine–Hydrazone Cu(II) Complexes, *Inorg. Chem.*, 2010, **49**, 5923–5934; (*c*) R. Clauss, S. Baweja, D. Gelman and E. Hey-Hawkins, Heterobimetallic Pd/Mn and Pd/Co complexes as efficient and stereoselective catalysts for sequential Cu-free Sonogashira coupling–alkyne semi-hydrogenation reactions, *Dalton Trans.*, 2021, **51**, 1344–1356.

18 D. Riou and G. Bouchoux, Protonation Thermochemistry of Gaseous 2,2′-, 4,4′-and 2,4′-Bipyridines and 1,10-phenanthroline, *Croat. Chem. Acta*, 2014, **87**, 447–457.

19 A.-M. Stadler, J. Ramirez and J.-M. Lehn, Control of Relative Direction and Amplitude in Extension/Contraction Motions of Molecular Strands Induced by Ion Binding, *Chem. – Eur. J.*, 2010, **16**, 5369–5378.

20 See, for example: (*a*) E. Kolomiets, V. Berl, I. Odriozola, A.-M. Stadler, N. Kyritsakas and J.-M. Lehn, Contraction/extension molecular motion by protonation/deprotonation induced structural switching of pyridine derived oligoamides, *Chem. Commun.*, 2003, 2868–2869; (*b*) C. Dolain, V. Maurizot and I. Huc, Protonation-Induced Transition between Two Distinct Helical Conformations of a Synthetic Oligomer via a Linear Intermediate, *Angew. Chem., Int. Ed.*, 2003, **42**, 2738–2740.

21 For an interesting example of protonation combined with coordination, see: A. Gasnier, J.-M. Barbe, C. Bucher, F. Denat, J.-C. Moutet, E. Saint-Aman, P. Terech and G. Royal, Acid–Base-Driven Interconversion between a Mononuclear Complex and Supramolecular Coordination Polymers in a Terpyridine-Functionalized Dioxocyclam Ligand, *Inorg. Chem.*, 2008, **47**, 1862–1864.